International Journal of Fluid Mechanics & Thermal Sciences
2026; 12(3): 51-61
http://www.sciencepublishinggroup.com/j/ijfmts
doi: 10.11648/j.ijfmts.20261203.11

Effect of Rayleigh Number on Double-Diffusive Natural Convection Flow in a Rectangular Enclosure

Peninnah Ngina Musili[1, *], Mark Okongo[2], Alice Lunani Mulama Murwayi[2]

[1]Faculty of Science and Technology, Chuka University, Meru, Kenya
[2]Department of Physical Sciences, Chuka University, Chuka, Kenya

Email address:
nginapenninah@gmail.com (Peninnah Ngina Musili), marikookongo@gmail.com (Mark Okongo),
almurwayi@yahoo.com (Alice Lunani Mulama Murwayi)

To cite this article:
Peninnah Ngina Musili, Mark Okongo, Alice Lunani Mulama Murwayi. (2026). Effect of Rayleigh Number on Double-Diffusive Natural Convection Flow in a Rectangular Enclosure. *International Journal of Fluid Mechanics & Thermal Sciences, 12*(3), 51-61.
https://doi.org/10.11648/j.ijfmts.20261203.11

Received: 6 June 2026; **Accepted:** 18 June 2026 **Published:** 4 September 2026

Abstract: Double diffusive natural convection driven by simultaneous temperature and concentration gradients is governed by the Rayleigh number Ra, which represents the balance between buoyancy and viscous forces. The Rayleigh number determines the transition from conduction-dominated to convection-dominated heat and mass transfer. While most existing studies rely on two-dimensional simplifications, this paper presents a three-dimensional numerical investigation of the effect of the Rayleigh number Ra on steady, laminar double-diffusive natural convection in a rectangular enclosure with an aspect ratio Ar of 0.5. The governing equations are solved using the finite volume method with the SIMPLE algorithm on a staggered grid. Parametric simulations are performed for $Ra = 10^4, 5 \times 10^4, 10^5$, and 10^6, with fixed Prandtl number $Pr = 7.0$, Lewis number $Le = 2.5$, and buoyancy ratio $N = 10$. The results reveal that increasing the Ra from 10^4 to 10^5 leads to a clear transition from conduction-dominated to convection-dominated heat and mass transfer. At $Ra = 10^4$, profiles are smooth, and gradients are weak; at $Ra = 10^5$, sharp boundary layers and strong circulation appear. Concentration profiles become sharper and more localized with increasing Ra. At high Ra, solutal stratification occurs, and solute remains confined near the source, indicating enhanced solutal buoyancy effects. Temperature profiles evolve from nearly parallel isotherms (conduction) to wavy, distorted patterns with thermal plumes (convection). Vertical heat transfer increases significantly with Ra. Velocity fields become stronger and more organized as Ra increases. At $Ra = 10^5$, well-defined primary and secondary circulation cells produce intense upwelling and downwelling, with velocities an order of magnitude higher than at low Ra. The 3-dimensional nature of the flow reveals anisotropy:the primary circulation plane (z-y) shows the strongest response, but secondary planes (x-y, x-z) also exhibit significant changes with Ra. These results provide valuable benchmarks for engineering applications where controlling the strength of buoyancy-driven convection is crucial, such as in solar collectors, building ventilation, and drying systems. The finite volume method proves to be an effective tool for such 3-dimensional parametric studies.

Keywords: Rayleigh Number, Double-Diffusive Convection, Finite Volume Method, 3D Flow, Heat and Mass Transfer

1. Introduction

Convection is a mode of heat transfer that occurs when a fluid flows over a solid surface of different temperature. When buoyancy forces arise from both temperature and concentration gradients, the phenomenon is termed double diffusive natural convection, which is central to many applications, including oceanography, building ventilation, drying of agricultural products, cooling of electronic devices, and chemical processing.

Rayleigh number Ra is defined as:

$$Ra = \frac{g\beta_T(T_h - T_l)L^3}{\alpha\nu}, \tag{1}$$

where g is gravitational acceleration, β_T is the thermal expansion coefficient, α is thermal diffusivity, ν is kinematic viscosity, and L is a characteristic length. It represents the relative strength of buoyancy to viscous forces. The onset of convection for Ra below a critical value (approx. $10^3 - 10^4$), heat transfer is dominated by conduction; above this, convection becomes dominant. Laminar flow regime occurs for $Ra < 10^9$ while turbulent flow regime occurs at higher Ra.

Early research by Veronis [1] and Turner [2] established the importance of the Rayleigh number alongside other dimensionless parameters. Mamou et al. [4] analytically and numerically studied double-diffusive convection in a vertical rectangular enclosure. They varied the Rayleigh number and reported its effect on Nusselt and Sherwood numbers. Their results showed good agreement between analytical predictions and numerical solutions, but the model remained two-dimensional. Mohamad & Bennacer [5] considered double-diffusive natural convection in an enclosure filled with a saturated porous medium. They compared two- and three-dimensional flows for Ra up to 10^5. While the flow exhibited three-dimensional structure, the differences in heat and mass transfer rates between two- dimensional (2-D) and three-dimensional (3-D) simulations were not significant because the spanwise flow was much weaker than the main flow. Their work highlighted that 3-D effects might be important for certain parameter ranges, motivating the present study. Belazizia et al. [11] studied the effect of Rayleigh number on thermal-solutal natural convection in a square enclosure with a top active vertical wall. Their numerical results showed that increasing Ra leads to an increase in heat and mass transfer rates. However, the study was limited to two dimensions. Ridha and Mounir [13] examined double-diffusive mixed convection in a double-lid driven rectangular cavity using the finite volume method. They found that convection heat transfer is more pronounced at a Rayleigh number of 10^6 and that increasing the buoyancy ratio also increased temperature. Their finite volume method (FVM) implementation was two-dimensional. Kuznetsov and Sheremet [9] analyzed the influence of Rayleigh number on fluid motion and heat/mass transfer in conjugate double-diffusive natural convection. They observed that higher Ra produces more intense flow and higher transfer rates.

Most prior numerical studies of double-diffusive convection have been confined to 2-D geometries and have employed finite difference or finite element methods. The finite volume method (FVM), known for its conservation properties and robustness, has received limited attention for 3-D parametric studies of Rayleigh number effects. Moreover, 3-D simulations are essential to capture the full spatial variation and cross-plane interactions that two-dimensional models miss.

This paper focuses specifically on the effect of varying the Rayleigh number on concentration, temperature, and velocity profiles in a steady, laminar, three-dimensional double-diffusive natural convection flow inside a rectangular enclosure. Using the FVM, we provide a comprehensive analysis of how increasing Ra from 10^4 to 10^6 influences the flow structure and transport phenomena.

2. Model Equations and Method of Solution

2.1. Physical Model and Assumptions

The study considers a rectangular enclosure of aspect ratio $AR = 0.5$ (height L, width and depth scaled accordingly). The left vertical wall ($x = 0$) is maintained at constant high temperature T_h and high concentration C_h. The opposite vertical wall ($x = W$) is at constant low temperature T_l and low concentration C_l. All other walls are adiabatic and impermeable. Gravity acts vertically downward (negative z-direction). The working fluid is a water-salt mixture.

The following assumptions are made:

1) The flow is three-dimensional, steady, and laminar.
2) The fluid is incompressible.
3) Gravitational acceleration acts only in the z-direction.
4) The Boussinesq approximation holds: density is constant except in the buoyancy term, where $\rho = 1 - \beta_T(T_h - T_l) + \beta_s(C_h - C_l)$.
5) Dufour and Soret effects are negligible.

2.2. Governing Equations

After non-dimensionalization using characteristic scales (length L, velocity U_0, temperature difference $\Delta T = T_h - T_l$, concentration difference $\Delta C = C_h - C_l$), the dimensionless governing equations are:

$$\frac{\partial u}{\partial x} + \frac{\partial v}{\partial y} + \frac{\partial w}{\partial z} = 0, \tag{2}$$

$$u\frac{\partial u}{\partial x} + v\frac{\partial u}{\partial y} + w\frac{\partial u}{\partial z} = -\frac{\partial p}{\partial x} + \frac{1}{Pr}\nabla^2 u, \tag{3}$$

$$u\frac{\partial v}{\partial x} + v\frac{\partial v}{\partial y} + w\frac{\partial v}{\partial z} = -\frac{\partial p}{\partial y} + \frac{1}{Pr}\nabla^2 v, \tag{4}$$

$$u\frac{\partial w}{\partial x} + v\frac{\partial w}{\partial y} + w\frac{\partial w}{\partial z} = -\frac{\partial p}{\partial z} + \frac{1}{Pr}\nabla^2 w + \frac{Ra}{Pr}(\theta - NC), \tag{5}$$

$$u\frac{\partial \theta}{\partial x} + v\frac{\partial \theta}{\partial y} + w\frac{\partial \theta}{\partial z} = \frac{1}{Pr}\nabla^2 \theta, \tag{6}$$

$$u\frac{\partial S}{\partial x} + v\frac{\partial S}{\partial y} + w\frac{\partial S}{\partial z} = \frac{1}{Le}\nabla^2 S. \tag{7}$$

The dimensionless parameters are: $Pr = \nu/\alpha$, $Ra = g\beta_T(T_h - T_l)L^3/(\alpha\nu)$, $Le = \alpha/D$, $N = \beta_c(C_h - C_l)/(\beta_T(T_h - T_l))$.

2.3. Parameter Ranges

The following fixed parameters were used: $Ar = 0.5$, $Pr = 7.0$ (water-salt mixture), $Le = 2.5$, $N = 10$. The Rayleigh number was varied in a range that spans the conduction-dominated regime ($Ra = 10^4$), the transition regime ($Ra = 5 \times 10^4$), and the convection-dominated regime ($Ra = 10^5$ and 10^6), while remaining within laminar flow bounds ($Ra < 10^9$).

2.4. Numerical Method: Finite Volume with SIMPLE

The governing partial differential equations are discretized using the finite volume method (FVM), which transforms the continuous equations into a system of algebraic equations by integrating over discrete control volumes. A key advantage of FVM is that it ensures conservation of mass, momentum, energy, and species over each control volume and hence over the entire domain.

2.4.1. Grid Generation and Staggered Arrangement

The three-dimensional domain (dimensions $L_x = L_y = L_z$ with AR=0.5) is subdivided into uniform rectangular control volumes. A general nodal point P is identified with its neighbors: East (E), West (W), North (N), South (S), Top (T), and Bottom (B). The control volume faces are denoted by lowercase letters e, w, n, s, t, b.

To avoid unphysical oscillatory pressure fields (checkerboard problem), a staggered grid is employed. Scalar variables (pressure p, temperature θ, concentration S) are stored at the main nodal points. Velocity components are stored on the cell faces: u velocities on the east and west faces, v velocities on the north and south faces, and w velocities on the top and bottom faces. This arrangement ensures that the pressure gradient driving a velocity component is evaluated across the same control volume for which that velocity is computed, providing a strong coupling between pressure and velocity.

2.4.2. Discretization of the Transport Equations

Applying the finite volume method to the x-momentum equation (as an example) over the u-control volume and using central differencing for diffusive fluxes yields a discretized equation of the form:

$$a_P u_{i,J,K} = \sum a_{nb} u_{nb} + (P_{I,J,K} - P_{I-1,J,K}) A_{i,J}, \quad (8)$$

where the summation index nb runs over the six neighboring velocity nodes $(i \pm 1, J, K;\ i, J \pm 1, K;\ i, J, K \pm 1)$. The coefficients a_{nb} contain contributions from convective and diffusive fluxes through the faces, and a_P is the sum of all neighboring coefficients plus any source terms. Similar discretized equations are obtained for the v- and w-momentum equations. The buoyancy term in the z-momentum equation becomes a source term that couples the temperature and concentration fields to the velocity field.

For the energy and concentration equations, which are scalar transport equations, the discretization is performed over the main (scalar) control volume, yielding:

$$a_P \phi_{I,J,K} = \sum a_{nb} \phi_{nb}, \quad (9)$$

where ϕ stands for θ or S. The coefficients depend on the velocity field, the Prandtl number (for energy), and the Lewis number (for concentration).

2.4.3. Pressure-Velocity Coupling: The SIMPLE Algorithm

The continuity equation does not contain an explicit pressure term. To link pressure and velocity, the Semi-Implicit Method for Pressure-Linked Equations (SIMPLE) algorithm is employed. The iterative procedure is as follows:

1) Guess the pressure field p^*.
2) Solve the momentum equations using p^* to obtain intermediate velocity components u^*, v^*, w^* from the discretized equations.
3) Compute pressure corrections p' such that $p = p^* + p'$. Velocity corrections u', v', w' are related to p' via simplified relations derived by dropping the neighboring velocity correction terms:

$$\begin{aligned} u' &= d_u(p'_{I-1,J,K} - p'_{I,J,K}), \\ v' &= d_v(p'_{I,J-1,K} - p'_{I,J,K}), \\ w' &= d_w(p'_{I,J,K-1} - p'_{I,J,K}). \end{aligned}$$

   Here d_u, d_v, d_w are geometric coefficients from the momentum discretization.
4) Substitute the corrected velocities $u = u^* + u'$, etc., into the discretized continuity equation. This yields a Poisson-like equation for the pressure correction p':

$$\begin{aligned} a_{I,J,K} p'_{I,J,K} &= a_{i+1,J,K} p'_{I+1,J,K} + a_{i-1,J,K} p'_{I-1,J,K} \\ &+ a_{I,j+1,K} p'_{I,J+1,K} + a_{I,j-1,K} p'_{I,J-1,K} \\ &+ a_{I,J,k+1} p'_{I,J,K+1} + a_{I,J,k-1} p'_{I,J,K-1} + b_{I,J,K}, \end{aligned}$$

   where the source term b contains the mass imbalance from the guessed velocities.
5) Solve the pressure correction equation (using a tri-diagonal matrix algorithm line by line) to obtain p'.
6) Update pressure and velocities: $p = p^* + \alpha_p p'$, $u = u^* + d_u(p'_{I-1,J,K} - p'_{I,J,K})$, etc., where α_p is an under-relaxation factor (typically 0.8 for pressure).
7) Solve the energy and concentration equations using the updated velocity field.
8) Check convergence: If residuals are above a tolerance (here 10^{-6}), return to step 2 with the corrected pressure as the new guess.

The algorithm is implemented in MATLAB. Under-relaxation is applied to all variables to ensure stability. The solution is considered converged when the normalized residuals for all equations fall below 10^{-6}. Grid independence was verified by refining the mesh from $30 \times 30 \times 30$ to $50 \times 50 \times 50$ and monitoring changes in the Nusselt and Sherwood numbers (less than 2% variation). The final results are presented on a $40 \times 40 \times 40$ grid.

3. Results and Discussion

3.1. Effect of Rayleigh Number on Concentration Profiles

3.1.1. Along the x-y Plane

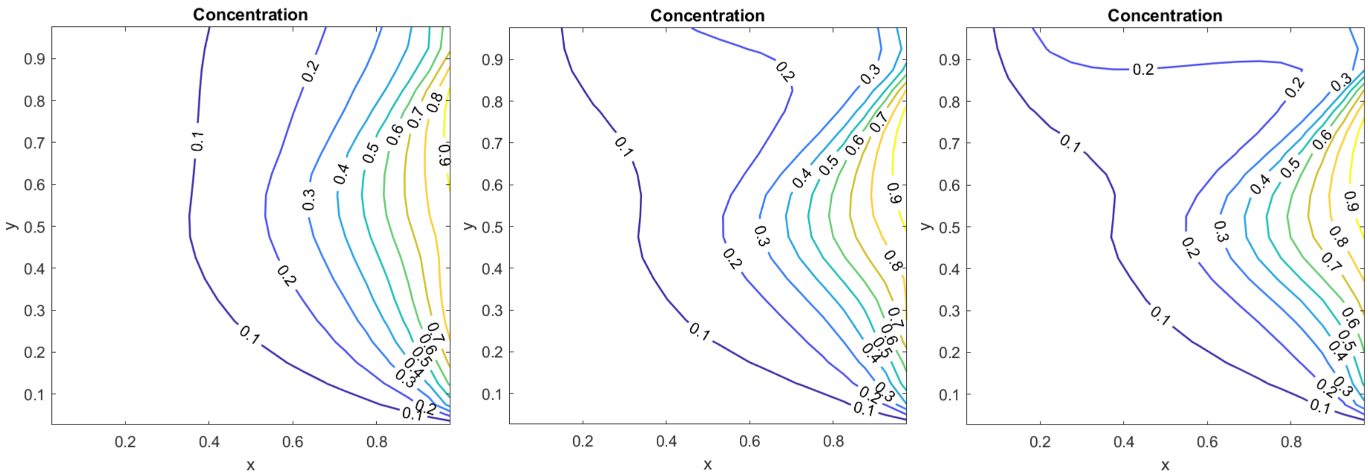

(a) $Ra = 10^4$ *(b)* $Ra = 5 \times 10^4$ *(c)* $Ra = 10^5$

Figure 1. *Effect of Rayleigh number on the concentration profile along x-y plane.*

The concentration profiles in Figure 1 show the distribution of solute within the enclosure, driven by buoyancy forces resulting from simultaneous temperature and concentration gradients. For all Rayleigh numbers, solute concentration decreases as fluid moves from the heated x-plane toward the cooler y-plane, indicating solutal transport due to buoyancy forces. The findings show that solutal transport strength increases with higher Rayleigh numbers, as buoyancy forces become more pronounced. This leads to more efficient mixing and redistribution of solute within the enclosure. At lower Rayleigh numbers ($Ra = 10^4$), the concentration gradients are smoother, and the solute distribution is more uniform. This indicates that conduction dominates over convection, resulting in weaker solutal transport. As the Rayleigh number increases ($Ra = 5 \times 10^4$ and 10^5), the concentration gradients become sharper, and the iso-concentration contours become more distinct. This suggests that convection becomes the dominant transport mechanism, enhancing solutal mixing. At higher Rayleigh numbers, secondary circulation patterns are observed, characterized by distinct concentration contours. These patterns are driven by stronger buoyancy forces, which create localized regions of solutal transport. The strength of solutal transport increases with higher Rayleigh numbers, as the buoyancy forces become more pronounced. This leads to more efficient mixing and redistribution of solute within the enclosure.

3.1.2. Along the x-z Plane

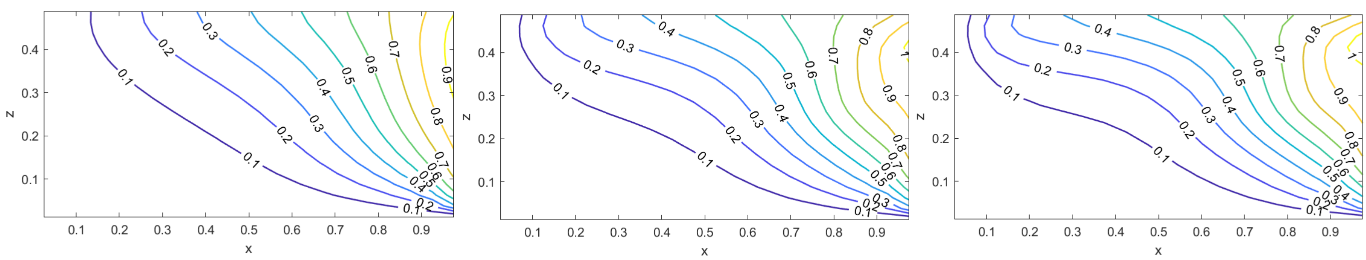

(a) $Ra = 10^4$ *(b)* $Ra = 5 \times 10^4$ *(c)* $Ra = 10^5$

Figure 2. *Effect of Rayleigh number on the concentration profile along x-z plane.*

The concentration profiles in Figure 2 show solutal transport from the heated x-plane toward the cooler z-plane, driven by buoyancy forces resulting from simultaneous temperature and concentration gradients. Results show that as the Rayleigh number increases, the buoyancy forces become stronger, driving more vigorous solutal transport. This results in sharper concentration gradients and more pronounced solutal circulation patterns. At lower Rayleigh numbers ($Ra = 10^4$), the concentration gradients are relatively smooth, indicating that conduction dominates over convection. The solute diffuses more uniformly across the enclosure. At higher Rayleigh numbers ($Ra = 5 \times 10^4$ and 10^5), the concentration gradients become sharper, and the isoconcentration contours are more distinct. This indicates that convection becomes the dominant transport mechanism, leading to stronger solutal mixinng. Results also show that at higher Rayleigh numbers, solutal transport becomes more localized, with distinct regions of high and low solute concentration forming within the enclosure. This indicates the development of secondary circulation patterns. The results highlight the impact of the Rayleigh number on concentration profiles along the x-z plane. Increasing the Rayleigh number leads to sharper concentration gradients, stronger solutal transport, and the formation of localized circulation patterns. These findings are essential for optimizing double-diffusive natural convection systems in engineering and environmental applications, where efficient solutal mixing is critical. This is consistent with [5].

3.1.3. Along the z-y Plane

Figure 3 is a representation of the Rayleigh number on the concentration profiles along the vertical-lateral (z-y) plane in a double-diffusive natural convection system. The results are represented using iso-concentration contours, which show the distribution of solute concentration across the enclosure. The profiles show solutal transport from the heated z-plane toward the cooler y-plane, driven by buoyancy forces resulting from simultaneous temperature and concentration gradients. This indicates primary circulation patterns along the z-y plane. Results show that at lower Rayleigh numbers ($Ra = 10^4$), the concentration gradients are smooth, and the solute distribution is relatively uniform. This indicates that conduction dominates over convection, resulting in weaker solutal transport.At higher Rayleigh numbers ($Ra = 5 \times 10^4$ and 10^5), the concentration gradients become sharper, and the isoconcentration contours are more distinct. This suggests that convection becomes the dominant transport mechanism, enhancing solutal mixing. This shows that as the Rayleigh number increases, the buoyancy forces become stronger, driving more vigorous solutal transport.

This results in sharper concentration gradients and more pronounced solutal circulation patterns. The results demonstrate the transition from conduction-dominated solutal transport at lower Rayleigh numbers to convection-dominated solutal transport at higher Rayleigh numbers.

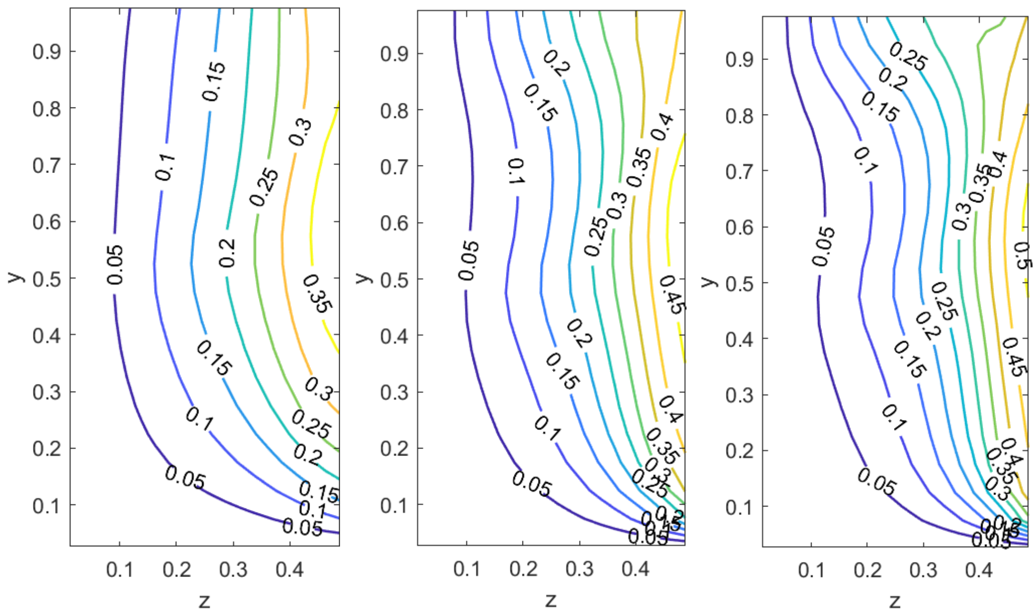

(a) $Ra = 10^4$ (b) $Ra = 5 \times 10^4$ (c) $Ra = 10^5$

Figure 3. *Effect of Rayleigh number on the concentration profile along z-y plane.*

3.2. Effect of Rayleigh Number on Temperature Profiles

3.2.1. Along the x-y Plane

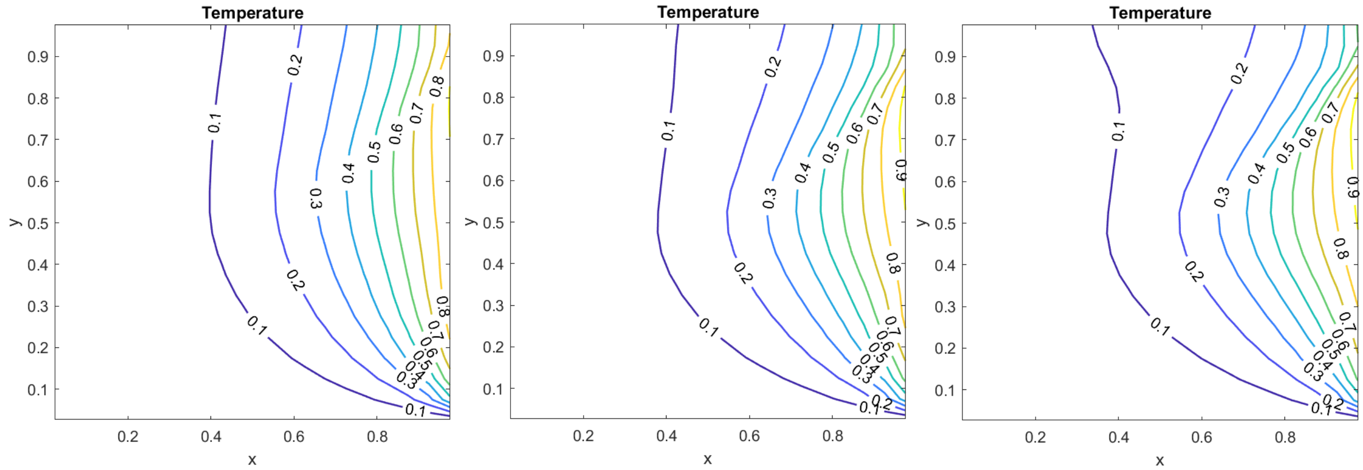

(a) $Ra = 10^4$ (b) $Ra = 5 \times 10^4$ (c) $Ra = 10^5$

Figure 4. *Effect of Rayleigh number on the temperature profile along x-y plane.*

Figure 4 is a representation of the effect of varying Rayleigh number on the temperature profiles along the horizontal-lateral (x-y) plane in an enclosure with double diffusive natural convection. The fluid flow in the enclosure is driven by a combined temperature and concentration gradient. The results are represented using isotherms, which connect points of equal temperature within the enclosure. The results highlight the impact of the Rayleigh number on temperature profiles along the x-y plane. Increasing the Rayleigh number leads to sharper temperature gradients, stronger secondary circulation, and enhanced heat transfer. At lower Rayleigh numbers ($Ra = 10^4$), the temperature gradients are smooth, indicating that conduction dominates over convection. Heat transfer is less vigorous, and the temperature distribution is relatively uniform. As the Rayleigh number increases ($Ra = 5 \times 10^4$ and 10^5), the temperature gradients become sharper, and the isotherms are more distinct. This suggests that convection becomes the dominant heat transfer mechanism, enhancing thermal mixing.

Results imply that higher Rayleigh numbers enhance heat transfer and mixing, The results also demonstrate a transition from conduction-dominated to convection dominated heat transfer as the Rayleigh number increases. This transition is critical for understanding the efficiency of thermal mixing in double-diffusive natural convection systems. The heat transfer dynamics indicate that at higher Rayleigh numbers, the buoyancy forces become stronger, driving more vigorous heat transfer. This results in sharper temperature gradients and more pronounced thermal circulation patterns. The temperature distribution becomes less uniform, with localized regions of high and low temperature forming within the enclosure. The results demonstrate a transition from conduction-dominated to convection-dominated heat transfer as the Rayleigh number increases. This transition is critical for understanding the efficiency of thermal mixing in double-diffusive natural convection systems. These observations agree with [11, 13].

3.2.2. Along the x-z Plane

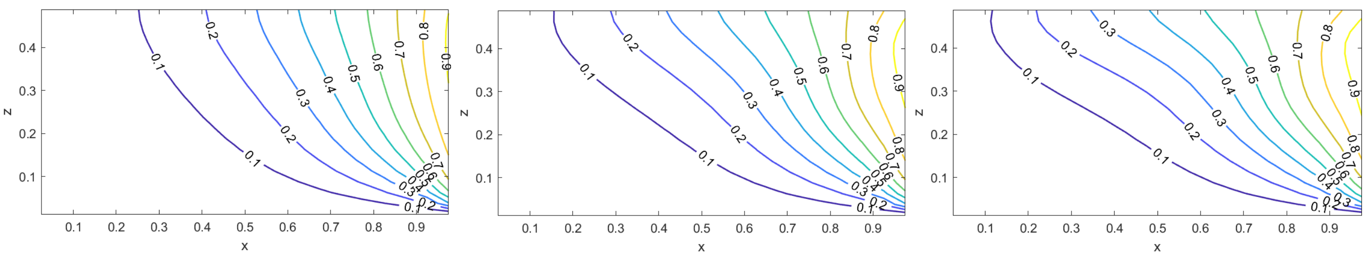

(a) $Ra = 10^4$ (b) $Ra = 5 \times 10^4$ (c) $Ra = 10^5$

Figure 5. *Effect of Rayleigh number on the temperature profile along x-z plane.*

Figure 5 is a representation of the effect of varying Rayleigh number on the temperature profiles along the horizontal-vertical (x-z) plane in an enclosure with double diffusive natural convection. The fluid flow in the enclosure is driven by a combined temperature and concentration gradient. The results are represented using isotherms, which connect points of equal temperature within the enclosure. The results highlight the impact of the Rayleigh number on temperature profiles along the x-z plane. Increasing the Rayleigh number leads to sharper temperature gradients, stronger vertical heat transfer, and the formation of localized circulation patterns. At lower Rayleigh numbers ($Ra = 10^4$), the temperature gradients are smooth, indicating that conduction dominates over convection. Heat transfer is less vigorous, and the temperature distribution is relatively uniform across the x-z plane. As the Rayleigh number increases ($Ra = 5 \times 10^4$ and 10^5), the temperature gradients become sharper, and the isotherms are more distinct. This indicates that convection becomes the dominant heat transfer mechanism, enhancing thermal mixing. The results also reveal a significant vertical heat transfer along the z-axis. For all Rayleigh numbers, buoyancy forces drive the less dense, heated air to rise along the z-plane, while denser, cooler air sinks. This vertical exchange becomes more pronounced as the Rayleigh number increases.

3.2.3. Along the z-y Plane

Figure 6 is a representation of the effect of varying Rayleigh number on the temperature profiles along the vertical-lateral (z-y) plane in an enclosure with double diffusive natural convection. The fluid flow in the enclosure is driven by a combined temperature and concentration gradient. The results are represented using isotherms, which connect points of equal temperature within the enclosure. The results highlight the impact of the Rayleigh number on temperature profiles along the z-y plane. Increasing the Rayleigh number leads to sharper temperature gradients, stronger vertical heat transfer, and the formation of localized circulation patterns. At lower Rayleigh numbers ($Ra = 10^4$), the temperature gradients are smooth, indicating that conduction dominates over convection. Heat transfer is less vigorous, and the temperature distribution is relatively uniform across the z-y plane. As the Rayleigh number increases ($Ra = 5 \times 10^4$ and 10^5), the temperature gradients become sharper, and the isotherms are more distinct. This suggests that convection becomes the dominant heat transfer mechanism, enhancing thermal mixing. Regarding vertical heat transfer, the results show significant heat transfer along the z-axis. At higher Rayleigh numbers, buoyancy forces drive the less dense, heated air to rise along the z-plane, while denser, cooler air sinks. This vertical exchange becomes more pronounced as the Rayleigh number increases.

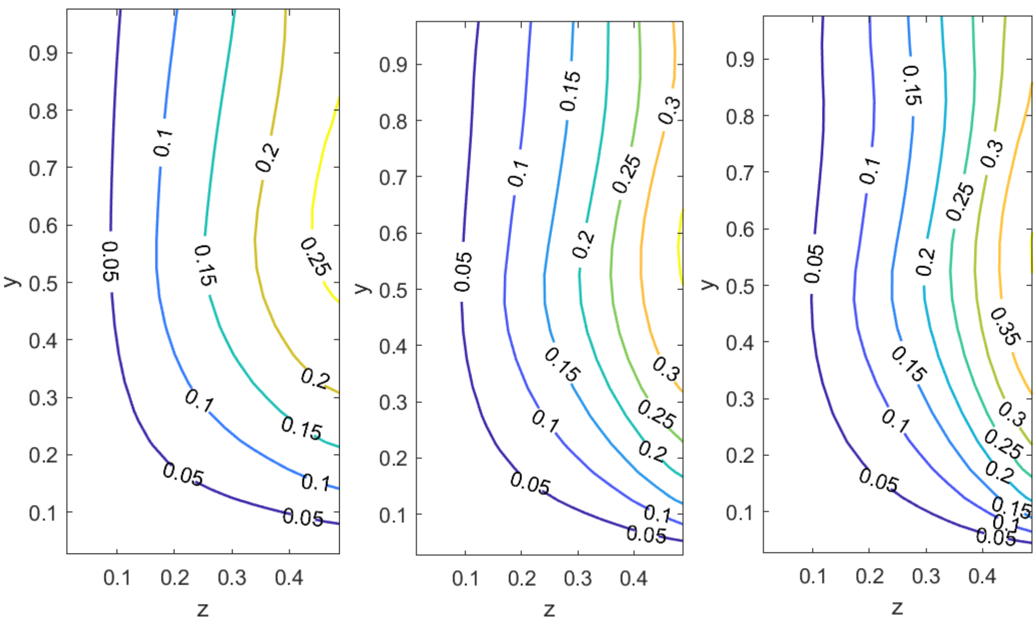

(a) $Ra = 10^4$ (b) $Ra = 5 \times 10^4$ (c) $Ra = 10^5$

Figure 6. Effect of Rayleigh number on the temperature profile along x-z plane.

3.3. Effect of Rayleigh Number on Velocity Profiles

3.3.1. Along the x-y Plane

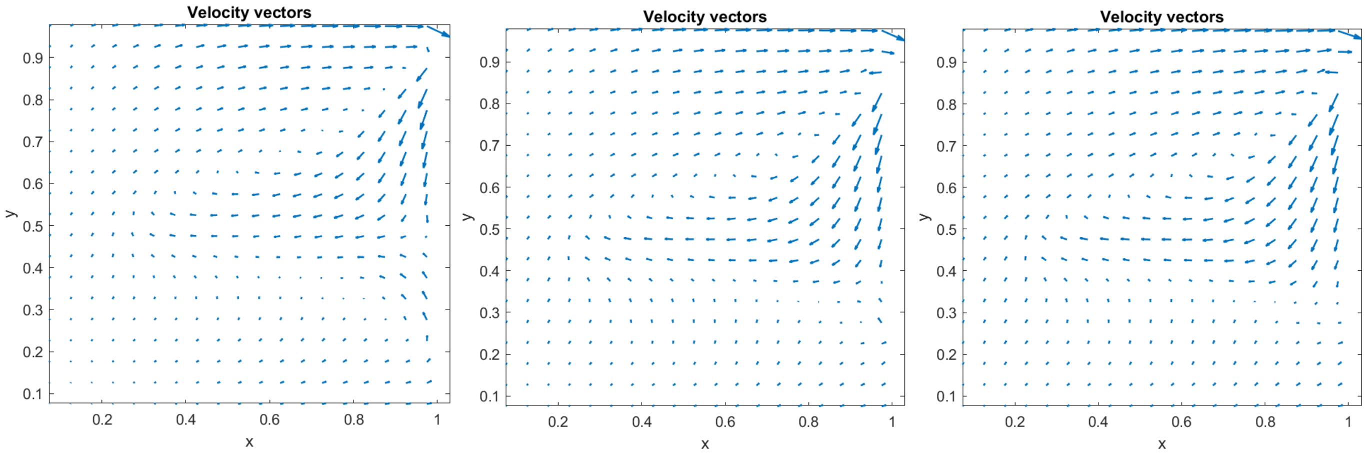

(a) $Ra = 10^4$ (b) $Ra = 5 \times 10^4$ (c) $Ra = 10^5$

Figure 7. *Effect of Rayleigh number on the velocity profiles along x-y plane.*

Figure 7 is a vector plot of the effect of varying the Rayleigh number on the velocity profiles along the horizontal-lateral (x-y) plane in an enclosure with double-diffusive natural convection. The results are represented using iso-concentrates, which depict the direction and magnitude of fluid flow within the enclosure. The figure shows the direction and magnitude of fluid flow within the enclosure. The velocity profiles reveal the formation of secondary circulation within the enclosure. This circulation is driven by buoyancy forces resulting from simultaneous temperature and concentration gradients. Fluid flows from the heated x-plane toward the cooler y-plane, with the returning flow near the enclosure boundaries. Results show that increasing Rayleigh numbers makes the secondary circulation more vigorous, with stronger velocity magnitudes and a more distinct flow pattern. At lower Rayleigh numbers $Ra = 10^4$), the velocity magnitudes are relatively small, and the flow patterns are less pronounced. This indicates that conduction dominates over convection, resulting in weaker fluid motion. As the Rayleigh number increases ($Ra = 5 \times 10^4$ and 10^5), the velocity magnitudes increase, and the flow patterns become more dynamic and organized. This suggests that convection becomes the dominant mechanism driving fluid motion. It is also revealed that at higher Rayleigh numbers, the flow becomes more streamlined, with well-defined circulation cells. This indicates that the system reaches a more stable and organized state as buoyancy forces dominate. The results also demonstrate the transition from conduction-dominated to convection dominated fluid motion as the Rayleigh number increases. This transition is critical for understanding the efficiency of fluid mixing in double-diffusive natural convection systems.

3.3.2. Along the x-z Plane

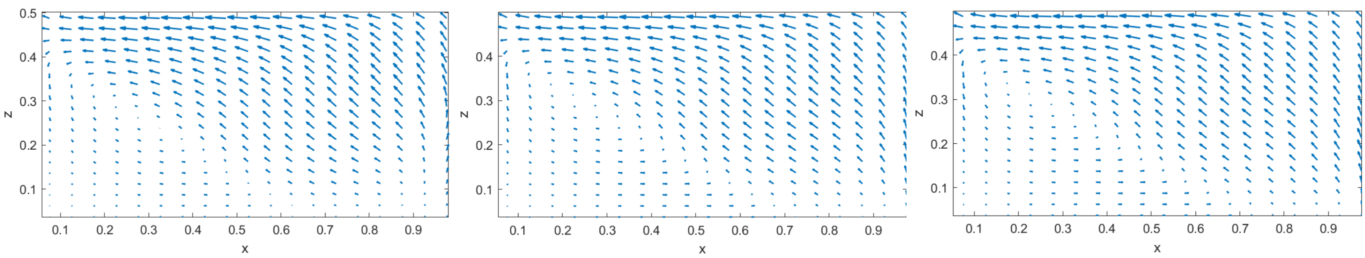

(a) $Ra = 10^4$ (b) $Ra = 5 \times 10^4$ (c) $Ra = 10^5$

Figure 8. *Effect of Rayleigh number on the velocity profiles along x-z plane.*

Figure 8 is a vector plot of the effect of varying the Rayleigh number on the velocity profiles along the horizontal-vertical (x-z) plane in an enclosure with double-diffusive natural convection. The results are represented using iso-concentrates, which depict the direction and magnitude of fluid flow within the enclosure. The figure shows the direction and magnitude of fluid flow within the enclosure. The velocity profiles reveal the formation of secondary circulation within the enclosure.

This circulation is driven by buoyancy forces resulting from simultaneous temperature and concentration gradients. Fluid flows from the heated z-plane toward the cooler x-plane, with the returning flow near the enclosure boundaries. Buoyancy forces drive the less dense, heated fluid to rise along the z-plane, while denser, cooler fluid sinks. This vertical exchange becomes more vigorous as the Rayleigh number increases.

Results indicate that with increasing Rayleigh numbers, the vertical circulation becomes more pronounced, with stronger velocity magnitudes and more distinct flow patterns. At lower Rayleigh numbers ($Ra = 10^4$), the velocity magnitudes are relatively small, and the flow patterns are less pronounced. This indicates that conduction dominates over convection, resulting in weaker fluid motion. As the Rayleigh number increases ($Ra = 5 \times 10^4$ and 10^5), the velocity magnitudes increase, and the flow patterns become more dynamic and organized. Convection becomes the dominant mechanism driving fluid motion. It is also observed that at higher Rayleigh numbers, the flow becomes more streamlined, with well-defined circulation cells. This indicates that the system reaches a more stable and organized state as buoyancy forces dominate. At higher Rayleigh numbers, the flow becomes more localized, with distinct regions of high and low velocity forming within the enclosure. This indicates the development of secondary circulation patterns and stratification. The results imply that higher Rayleigh numbers lead to stronger vertical fluid motion, which enhances mixing and heat transfer along the x-z plane.

3.3.3. Along the z-y Plane

Figure 9 is a vector plot of the effect of varying the Rayleigh number on the velocity profiles along the vertical - horizontal (z-y) plane in an enclosure with double-diffusive natural convection. The results are represented using iso-concentrates, which depict the direction and magnitude of fluid flow within the enclosure. The figure shows the direction and magnitude of fluid flow within the enclosure. The velocity profiles reveal the formation of primary circulation within the enclosure. This circulation is driven by buoyancy forces resulting from simultaneous temperature and concentration gradients. Fluid flows from the heated z-plane toward the cool yplane, with the returning flow near the enclosure boundaries. Buoyancy forces drive the less dense, heated fluid to rise along the z-plane, while denser, cooler fluid sinks.

This vertical exchange becomes more vigorous as the Rayleigh number increases. Results show that increasing the Rayleigh number leads to more organized circulation patterns and enhanced mixing and heat transfer. At lower Rayleigh numbers ($Ra = 10^4$), the velocity magnitudes are relatively small, and the flow patterns are less pronounced, indicating that conduction dominates over convection. As the Rayleigh number increases ($Ra = 5 \times 10^4$ and 10^5), the velocity magnitudes increase significantly, and the flow patterns become more dynamic and organized. Convection becomes the dominant mechanism driving fluid motion. Vertical fluid movement is also observed. The velocity profiles show significant vertical fluid movement along the z-axis. Buoyancy forces drive the less dense, heated fluid to rise along the z-plane, while denser, cooler fluid sinks. This vertical exchange becomes more vigorous as the Rayleigh number increases. Localized flow dynamics are also observed. At higher Rayleigh numbers, the flow becomes more localized, with distinct regions of high and low velocity forming within the enclosure. This indicates the development of stratified layers and primary circulation patterns.

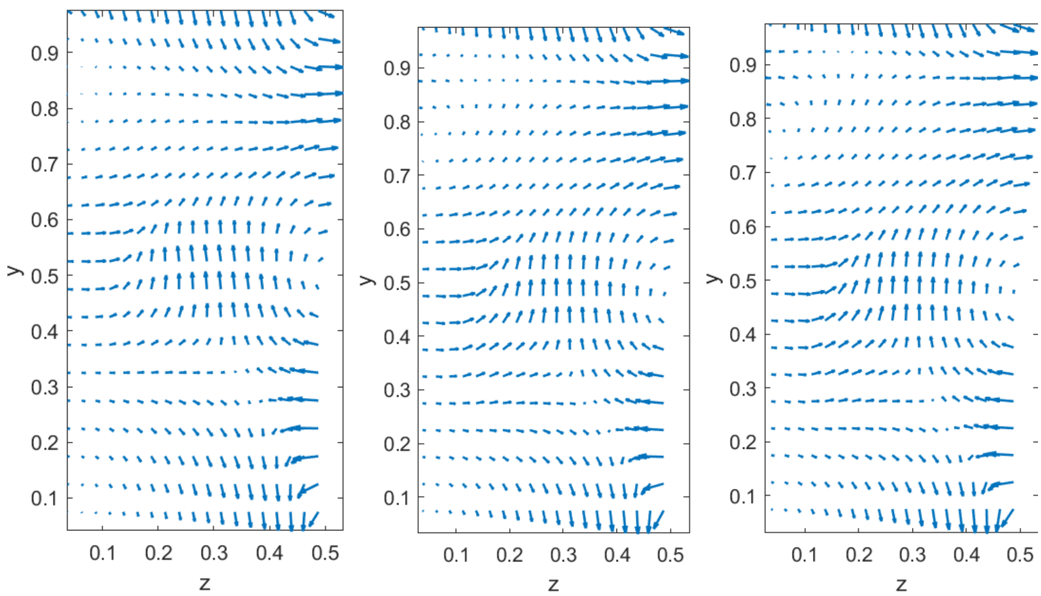

(a) $Ra = 10^4$ *(b) $Ra = 5 \times 10^4$* *(c) $Ra = 10^5$*

***Figure 9.** Effect of Rayleigh number on the velocity profiles along z-y plane.*

4. Conclusion

This paper presents a three-dimensional numerical study of the effect of the Rayleigh number Ra on concentration, temperature, and velocity profiles in steady, laminar double-diffusive natural convection within a rectangular enclosure (AR = 0.5). The finite volume method with SIMPLE algorithm was used to solve the coupled governing equations. The main conclusions are:

1) Increasing the Rayleigh number from 10^4 to 10^5 leads to a clear transition from conduction-dominated to convection-dominated heat and mass transfer. At $Ra = 10^4$, profiles are smooth and gradients are weak; at $Ra = 10^5$, sharp boundary layers and strong circulation appear.
2) Concentration profiles become sharper and more localized with increasing Ra. At high Ra, solutal stratification occurs, and solute remains confined near the source, indicating enhanced solutal buoyancy effects.
3) Temperature profiles evolve from nearly parallel isotherms (conduction) to wavy, distorted patterns with thermal plumes (convection). Vertical heat transfer increases significantly with Ra.
4) Velocity fields become stronger and more organized as Ra increases. At $Ra = 10^5$, well-defined primary and secondary circulation cells produce intense upwelling and downwelling, with velocities an order of magnitude higher than at low Ra.
5) The 3D nature of the flow reveals anisotropy: the primary circulation plane (z-y) shows the strongest response, but secondary planes (x-y, x-z) also exhibit significant changes with Ra.

These results provide valuable benchmarks for engineering applications where controlling the strength of buoyancy-driven convection is crucial, such as in solar collectors, building ventilation, and drying systems. The finite volume method proves to be an effective tool for such 3D parametric studies.

Future work should extend the analysis to unsteady and turbulent regimes (higher Ra), include Soret and Dufour effects, and explore the interaction of Rayleigh number with aspect ratio and other dimensionless parameters.

ORCID

0009-0001-0901-7381 (Peninnah Ngina Musili)

Abbreviations

MATLAB	Matrix Laboratory
FVM	Finite Volume Method
AR	Aspect Ratio
Cp	Specific Heat Capacity at Constant Pressure $jKg^{-1}K^{-1}$
g	Gravitational Acceleration ms^{-1}
T	Temperature K
P	Thermodynamic Pressure Nm^2
t	Time s
h	Hot Wall and High Concentration
c	Cold Wall and Low Concentration
u, v	Velocity Components
x, y	Dimensional Coordinates
Pr	Prandtl Non- dimensional Number
Ra	Rayleigh Non- dimensional Number
Sc	Schmidt Non -dimensional Number
Le	Lewis Non -dimensional Number
α	Thermal Diffusivity m^2s^{-1}
ρ	Density Kgm^{-3}
Ï	Kinematic Viscosity m^2s^{-1}
β	Thermal Expansion Coefficient K^{-1}
D	Mixture Average Diffusion Coefficient
λ	Thermal Conductivity

Acknowledgments

The authors gratefully acknowledge Chuka University for providing computational facilities and academic support. Special thanks to colleagues in the Department of Physical Sciences for constructive discussions that enriched this work.

Author Contributions

Peninnah Ngina Musili: Conceptualization, Formal Analysis, Methodology, Software Visualization, Writing – original draft, Writing – review & editing

Mark Okongo: Project administration, Supervision, Validation

Alice Lunani Mulama Murwayi: Project administration, Supervision, Validation

Conflicts of Interest

The authors declare no conflict of interest.

References

[1] Veronis, G. (1965). On finite amplitude instability in thermohaline convection. *Journal of Marine Research*, 23, 1-17.

[2] Turner, J. S. (1965). The coupled turbulent transports of salt and heat across a sharp density interface. International Journal of Heat and Mass Transfer, 8(5), 759-767. https://doi.org/10.1016/0017-9310(65)90022-0

[3] Ho, C. J., & Chang, J. Y. (1994). A study of natural convection heat transfer in a vertical rectangular enclosure with two-dimensional discrete heating: Effect of aspect ratio. International Journal of Heat and Mass Transfer, 37(6), 917-925. https://doi.org/10.1016/0017-9310(94)90217-8

[4] Mamou, M., Vasseur, P., & Bilgen, E. (1996). Analytical and numerical study of double diffusive convection in a vertical enclosure. Heat and Mass Transfer, 32(1-2), 115-125. https://doi.org/10.1007/s002310050100

[5] Mohamad, A. A., & Bennacer, R. (2002). Double-diffusion natural convection in an enclosure filled with a saturated porous medium. Numerical Heat Transfer, Part A: Applications, 41(5), 453-470. https://doi.org/10.1080/10407780290059564

[6] Costa, V. A. F. (2004). Double-diffusive natural convection in parallelogrammic enclosures. International Journal of Heat and Mass Transfer, 47(14-16), 2913-2926. https://doi.org/10.1016/j.ijheatmasstransfer.2004.02.013

[7] Bilgen, E., & Yedder, R. B. (2007). Natural convection in enclosure with heating and cooling by sinusoidal temperature profiles on one side. International Journal of Heat and Mass Transfer, 50(1-2), 139-150. https://doi.org/10.1016/j.ijheatmasstransfer.2006.06.027

[8] Abu-Nada, E., Masoud, Z., Oztop, H. F., & Campo, A. (2010). Effect of nanofluid variable properties on natural convection in enclosures. International Journal of Thermal Sciences, 49(3), 479-491. https://doi.org/10.1016/j.ijthermalsci.2010.07.006 *International Journal of Thermal Sciences*, 49(3), 479-491.

[9] Kuznetsov, G. V., & Sheremet, M. A. (2011). Natural convection in an enclosure with double diffusive conjugate natural convection. International Journal of Heat and Mass Transfer, 54(1-3), 456-465. https://doi.org/10.1016/j.ijheatmasstransfer.2010.09.033

[10] Anderson, D., Tannehill, J. C., Pletcher, R. H., Munipalli, R., & Shankar, V. (2020). Computational Fluid Mechanics and Heat Transfer. CRC Press.

[11] Belazizia, A., Benissaad, S., & Abboudi, S. (2012). Double-diffusion natural convection of binary fluid in a square enclosure with top active vertical wall. *Advances in Theoretical and Applied Mechanics*, 5(3), 119-131.

[12] Elsherbiny, S. M., & Ragab, E. H. (2013). Laminar natural convection in inclined rectangular cavities with a localized heat source. Alexandria Engineering Journal, 52(3), 249-257. https://doi.org/10.1016/j.aej.2012.12.004

[13] Ridha, B., & Mounir, B. (2014). Effect of buoyancy ratio on double-diffusive mixed convection in a double-lid driven rectangular cavity. Heat Transfer Engineering, 35(5), 456-467. https://doi.org/10.1080/01457632.2013.819539

[14] Falahat, A. (2014). Effect of aspect ratio on laminar natural convection in a partially heated enclosure. Universal J. Mech. Eng, 2(1), 28-33.

[15] Aly, A. M., & Raizah, Z. A. (2016). Double-diffusive natural convection in an enclosure filled with nanofluid using ISPH method. Alexandria Engineering Journal, 55(4), 3037-3052. https://doi.org/10.1016/j.aej.2016.07.004

[16] Aghighi, M., Ammar, A., & Masoumi, H. (2022). Double-diffusive natural convection of Casson fluids in an enclosure. International Journal of Mechanical Sciences, 236, 107754. https://doi.org/10.1016/j.ijmecsci.2022.107754